

Adsorption and Thermal Reactions of Alkanethiols on Pt(111): Dependence on the Length of the Alkyl Chain

T. H. Lin,[†] T. P. Huang,[†] Y. L. Liu,[†] C. C. Yeh,[‡] Y. H. Lai,[‡] and W. H. Hung^{*,†,‡}

Department of Chemistry, National Taiwan Normal University, Taipei 116, Taiwan, and
National Synchrotron Radiation Research Center, Hsinchu 300, Taiwan

Received: March 7, 2005

The adsorption and thermal decomposition of alkanethiols ($R-SH$, where $R = CH_3$, C_2H_5 , and C_4H_9) on Pt(111) were studied with temperature-programmed desorption (TPD) and X-ray photoelectron spectroscopy (XPS) with synchrotron radiation. Dissociation of sulfhydryl hydrogen ($RS-H$) of alkanethiol results in the formation of alkanethiolate; the extent of dissociation at an adsorption temperature of 110 K depends on the length of the alkyl chain. At small exposure, all chemisorbed CH_3SH , C_2H_5SH , and C_4H_9SH decompose to desorb hydrogen below 370 K and yield carbon and sulfur on the surface. Desorption of products containing carbon is observed only at large exposure. In thermal decomposition, alkanethiolate is proposed to undergo a stepwise dehydrogenation: $R'-CH_2S \rightarrow R'-CHS \rightarrow R'-CS$, $R' = H$, CH_3 , and C_3H_7 . Further decomposition of the $R'-CS$ intermediate results in desorption of H_2 at 400–500 K and leaves carbon and sulfur on the surface. On the basis of TPD and XPS data, we conclude that the density of adsorption of alkanethiol decreases with increasing length of the alkyl chain. C_4H_9SH is proposed to adsorb mainly with a configuration in which its alkyl group interacts with the surface; this interaction diminishes the density of adsorption of alkanethiols but facilitates dehydrogenation of the alkyl group.

Introduction

From the point of view of industrial importance, the adsorption and thermal decomposition of alkanethiols on platinum metal are of interest for several reasons. First, because these thiols are commonly found in crude oil,^{1,2} the thermal reaction of alkanethiols on surfaces is associated with poisoning of Pt-based catalysts used to reform hydrocarbons. The second involves the preparation of a self-assembled monolayer on a metallic surface, which can modify the chemical and physical properties of surfaces and which is potentially adaptable for various applications such as wetting, passivation, and protection;^{3–5} self-assembled monolayers of alkanethiolate are reported to be formed on the surface of a Pt film.^{6–9} According to results from infrared spectra in reflection and absorption, the tilt angle of the alkyl chain is estimated to be less than 15° .¹⁰ Third, thiols serve to stabilize or to functionalize Pt nanoparticles with desirable properties.¹¹

Previous workers have shown that the species CH_xS with $x \leq 3$ are formed upon adsorption and sequential dehydrogenation of CH_3SH on Pt(111).¹² Data from measurements of near-edge X-ray absorption fine structure indicate that the angle of the C–S bond to the surface is altered with the extent of dehydrogenation.^{13,14} We report here an investigation, utilizing thermally programmed desorption (TPD) and X-ray photoelectron spectroscopic (XPS) techniques, of the mechanism of adsorption and decomposition of methanethiol on a Pt(111) surface; thereby, we have elucidated the pathways of the surface reaction. In principle, the length of the carbon chain of an alkanethiol might exert a significant influence on its thermal stability and

reaction mechanism through the presence of β -hydrogens and the interaction between the metallic surface and the alkyl group.^{15–22} We thus undertook a comparison of thermal reactivity and reaction products for alkanethiols with varied length of alkyl chain, that is, RSH with $R = CH_3$, C_2H_5 , and C_4H_9 , thus probing the formation and thermal decomposition of an alkanethiolate adlayer on the Pt surface. This work provides mechanistic insight into the deposition of sulfur on a catalytic surface of Pt and serves as a useful reference for the adsorption of alkanethiols with longer carbon chains.

Experiments

Experiments were performed in an UHV chamber (base pressure $\sim 2 \times 10^{-10}$ Torr) that was equipped with a quadrupole mass filter (EPIC, Hiden) and an electron-energy analyzer (HA100, VSW). A Pt(111) sample was spot-welded on two Ta wires that were in turn mounted on a copper block. The Pt sample could be cooled to 110 K with liquid nitrogen via conduction through the copper block and heated resistively. The Pt(111) surface was cleaned through Ar^+ sputtering, followed by thermal annealing to 1000 K in an oxygen atmosphere ($\sim 10^{-7}$ Torr) to remove residual carbon from the surface. When the surface was further annealed to 1200 K, it exhibited XPS features characteristic of clean Pt, with no evidence for either carbon or oxygen being present.

Before use, C_2H_5SH (>99%, Merck), C_4H_9SH (>98%, Merck), and $(CH_3)_3CSH$ (>99%, Merck) liquids were subjected to several freeze–pump–thaw cycles. CH_3SH (>99.5%, Matheson) was used without further purification. Alkanethiols were introduced onto the Pt surface with a doser having a pinhole of diameter 250 μm . During dosing, the partial pressures of alkanethiols were controlled at 5×10^{-10} Torr and the sample surface was placed ~ 2 cm before the doser pinhole to minimize contamination of the UHV system with thiols.

* Corresponding author. E-mail: whung@cc.ntnu.edu.tw. Fax: +886-2-2934249.

[†] National Taiwan Normal University.

[‡] National Synchrotron Radiation Research Center.

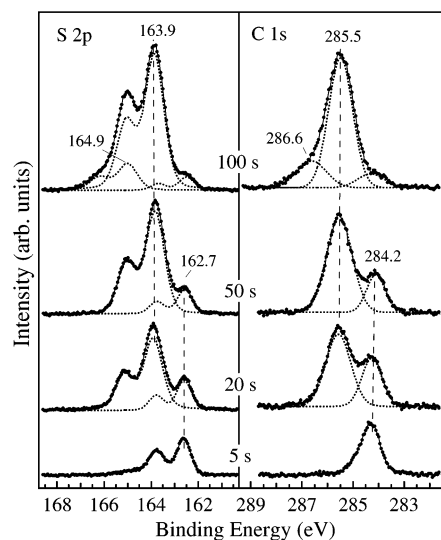


Figure 1. XPS spectra of S 2p and C 1s recorded for a Pt surface after exposure to CH_3SH for varied durations at 110 K. Dotted lines represent data collected after background subtraction, which are fitted with various components shown as dashed lines. The photon energy used to collect these spectra is 380 eV.

XPS measurements were conducted at the wide-range beam-line of National Synchrotron Radiation Research Center in Taiwan; the incident angle of the photon beam was 45° from the surface normal. Emitted photoelectrons were collected with an electron analyzer oriented 10° from the surface normal in an angle-integrated mode. For measurements at varied temperatures, the sample was heated to a desired temperature at a rate of 1 K/s and cooled immediately to 110 K, at which time XPS spectra were recorded. Collected spectra were numerically fitted with Gaussian-broadened Lorentzian functions after Shirley background subtraction with a third-order polynomial to each side of a peak in all fits. Alkanethiols are highly sensitive to X-radiation and can undergo photodissociation during XPS measurement; to suppress interference resulting from photodissociation, we completed the recording of each XPS spectrum within 2 min, and the probed area of the surface was changed after each XPS measurement.

The quadrupole mass filter rendered analysis of desorption products in the TPD measurement. The mass analyzer was enclosed in a differentially pumped cylinder, at the end of which is a skimmer with an entrance aperture with a diameter of 2 mm. For TPD measurement, the sample surface was placed about 2 mm before the aperture and in line of sight of the ionizer of the mass filter; TPD spectra were recorded upon ramping the sample at a linear rate of ~ 2 K/s.

Results and Discussion

We applied XPS measurements to characterize the chemical identity of surface species upon the adsorption and thermal fragmentation of CH_3SH on a Pt surface. Figure 1 shows XPS spectra of S 2p and C 1s collected from a Pt(111) surface exposed to CH_3SH at 110 K for varied duration. Three S $2p_{3/2}$ features appear at 162.7, 163.9, and 164.9 eV in order of increasing duration of exposure. The first feature, dominant at small exposures, is attributed to methanethiolate (CH_3S) and the second feature is due to chemisorbed CH_3SH . CH_3S is formed upon deprotonation of the sulfhydryl group, $\text{CH}_3\text{SH} \rightarrow \text{CH}_3\text{S} + \text{H}$, as is observed on other metallic surfaces.¹⁹ The CH_3S is believed to bind to the surface with a tilted off-top adsorption geometry in which the S atom is located at a site

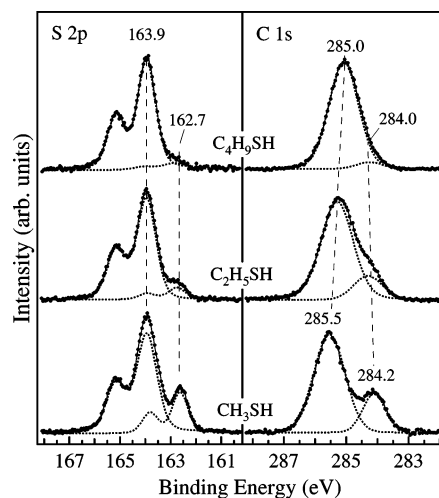


Figure 2. Comparison of S 2p and C 1s spectra for a Pt surface saturated with CH_3SH , $\text{C}_2\text{H}_5\text{SH}$, and $\text{C}_4\text{H}_9\text{SH}$ at 110 K.

near the face-centered cubic (fcc) hollow of the Pt(111) surface.^{23,24} With a duration of exposure greater than 50 s, the intensity of the feature at 163.9 eV increases with exposure, whereas the intensity of that at 162.7 eV due to CH_3S is attenuated. This observation indicates that physisorbed CH_3SH accumulates on the surface with a S 2p binding energy similar to that of chemisorbed CH_3SH . Moreover, an additional S $2p_{3/2}$ feature develops at 164.9 eV in the presence of physisorbed CH_3SH . This feature indicates that a fraction of condensed CH_3SH molecules are assembled with hydrogen bonding that induces an increased binding energy of the core-level electrons of S 2p.^{25,26} This feature is absent from the physisorption of $\text{C}_2\text{H}_5\text{SH}$ and $\text{C}_4\text{H}_9\text{SH}$. The formation of hydrogen bonding of physisorbed alkanethiol depends on the acidity of the sulfhydryl group. Figure 1 also shows that three corresponding C 1s chemical states of methyl groups are observed at 284.2, 285.5, and 286.6 eV. The first two features are attributed to dissociated CH_3S and to chemisorbed and physisorbed CH_3SH molecules, respectively.

Figure 2 shows a comparison of S 2p and C 1s spectra for a Pt surface saturated with CH_3SH or $\text{C}_2\text{H}_5\text{SH}$ or $\text{C}_4\text{H}_9\text{SH}$ at 110 K. Two C 1s features are obtained at ~ 284.2 and 285.0 – 285.5 eV; the first feature corresponds to alkanethiolate, and the second feature is attributed to chemisorbed alkanethiol, which shifts toward decreased binding energy with increased length of the alkyl chain. The ratio of S 2p intensities at 162.7 and 163.9 eV indicates the extent of dissociation of alkanethiol to form alkanethiolate. If the integrated area of each XPS component is proportional to the proportion of corresponding species, 15–20% of adsorbed CH_3SH dissociates to form CH_3S at 110 K. In contrast to the case of CH_3SH , adsorbed $\text{C}_4\text{H}_9\text{SH}$ deprotonates to only a small fraction to form thiolate at 110 K. The alkanethiol with a longer alkyl chain adsorbs with a smaller extent of dissociation. Thus, the dissociation of alkanethiol depends also on the acidity of the sulfhydryl group.

Figures 3 and 4 show TPD spectra recorded for a Pt surface exposed to CH_3SH at 110 K for varied durations. H_2 ($m/e = 2$) and CH_4 ($m/e = 16$) are the desorption products of the decomposition of CH_3SH . The desorption of physisorbed CH_3SH ($m/e = 48$) is observed at 125 K for a duration of exposure greater than 50 s. At small exposure, a desorption feature of H_2 is observed at 295 K, and a second feature appears at 270 K with increased exposure. The desorption state at 295 K gradually disappears, and an additional desorption feature appears at 225 K for exposure durations greater than 30 s. These desorption

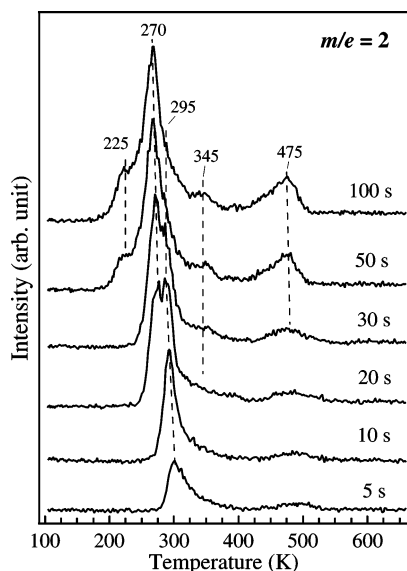


Figure 3. TPD spectra of H_2 ($m/e = 2$) for a Pt(111) surface exposed to CH_3SH at 110 K as a function of duration of exposure.

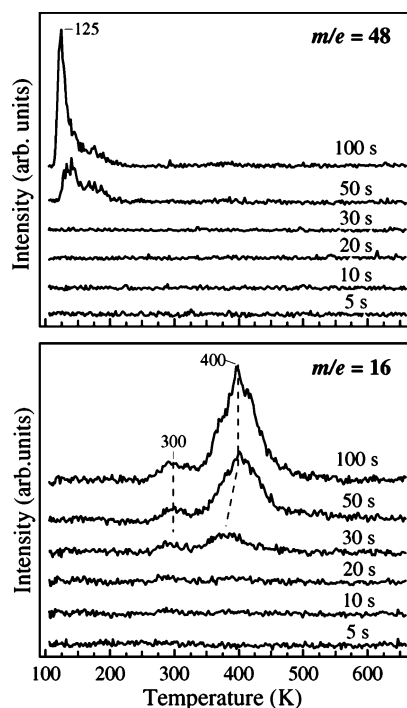


Figure 4. TPD spectra of CH_4 ($m/e = 16$) and CH_3SH ($m/e = 48$) for a Pt(111) surface exposed to CH_3SH at 110 K as a function of duration of exposure.

features resemble those obtained upon the adsorption of H_2S .^{27–29} For the decomposition of H_2S , the desorption of hydrogen depends on coverage because the dissociated sulfur and hydrogen compete for adsorption sites. Hence, the desorption states of H_2 observed upon the decomposition of CH_3SH are attributed to the combinative reaction of surface hydrogen that binds to various sites. At small coverage, CH_3SH decomposes completely to produce surface hydrogen on an adsorption site, which subsequently desorbs with a maximum at 295 K. At large coverage, the corresponding site is preferentially occupied by chemisorbed CH_3SH and CH_3S via the S atom;^{24,26,30} thus, hydrogen formed by sequential decomposition adsorbs on other sites with smaller binding energies, which results in the desorption states at 270 and 220 K. For comparison, we investigated the decomposition of dimethyl disulfide ($\text{H}_3\text{-}$

CSSCH_3) on a Pt(111) surface.³¹ H_2 and CH_4 are also desorption products: their desorption features are similar to those observed in the case of CH_3SH , because the CH_3S intermediate is also formed upon cleavage of the weak $\text{H}_3\text{CS-SCH}_3$ bond during thermal decomposition.

On the basis of vibrational spectra, the species CH_2S and CHS have been proposed to be intermediates during the thermal decomposition of CH_3S on Pt at 225 and 475 K, respectively.¹² As is generally known, platinum metal acts as an effective catalyst for the dehydrogenation of hydrocarbon because the interaction of Pt and H atoms facilitates breaking the C–H bond.³² At small coverage, most CH_3S completely dehydrogenates to form surface hydrogen, as shown in Figure 3. With further increasing exposure, H_2 and CH_4 are decomposition products of CH_3SH , whereas signals of species with longer carbon chains (e.g., C_2H_4) are less than our detection limit, in contrast to a previous report.¹² The desorption of CH_4 exhibits an intense maximum at 400 K with a shoulder at 300 K. At large coverage, the catalytic activity for dehydrogenation on a Pt surface is diminished because adsorption sites are occupied mostly by CH_xS . Hence, the CH_x moiety of CH_xS disproportionates to form CH_4 . The desorption feature at 300 K is analogous to that observed for surface CH_3 that is formed upon thermal desorption of CH_3I .^{33,34} Thus, the CH_3S intermediate dissociates to a small extent to form surface CH_3 and S at large coverage.

In contrast, a large fraction of CH_3S might initially dehydrogenate to CH_2S at a temperature below 240 K.³¹ The catalytic activity of surface Pt for further dehydrogenation of CH_2S is diminished because neighboring empty sites become fewer with increasing duration of exposure or coverage. Breaking of the C–H bond in CH_2S to form CHS begins at ~ 320 K, which is a temperature significantly higher than that at which the desorption of surface hydrogen occurs. Thus, a fraction of CH_2S undergoes dehydrogenation that results in a small desorption feature of H_2 at 345 K, as shown in Figure 3. We believe, however, that breaking of the C–S bond in CH_2S is also activated in this temperature range and initiates the disproportionation of CH_2 moieties. This disproportionation results in the desorption of CH_4 with a maximum at 400 K and then the formation of S adatoms and CHS : $\text{CH}_2\text{S} \rightarrow \text{CH}_4 + \text{S} + \text{CHS}$. The desorption of H_2 at 475 K is attributed to originate from further dehydrogenation of the CHS species. A similar feature of the desorption of H_2 is observed in the temperature range 450–500 K for the decomposition of $\text{C}_2\text{H}_5\text{SH}$ and $\text{C}_4\text{H}_9\text{SH}$ but with a great difference in their relative intensities, which is discussed below.

Figure 5 shows the thermal evolution of S 2p and C 1s spectra for a Pt surface exposed to CH_3SH at 110 K for 100 s. At 130 K, the S 2p_{3/2} at 164.9 eV and C 1s at 286.6 eV components due to a condensed CH_3SH multilayer with hydrogen bonding disappear because of molecular desorption, as shown in TPD data. At 170 K, the S 2p_{3/2} feature at 163.9 eV and the C 1s feature at 285.5 eV due to chemisorbed CH_3SH disappear, whereas the intensities of S 2p_{3/2} at 162.2 eV and C 1s at 284.2 eV increase, indicating that all chemisorbed CH_3SH molecules deprotonate to form CH_3S . Between 250 and 320 K, the S 2p and C 1s features become broad and gradually shift toward smaller binding energy. According to the previous argument, these spectral changes reflect the dehydrogenation of the CH_3S species into CH_2S with S 2p_{3/2} at 162.2 eV and C 1s at 283.8 eV. Upon heating the sample to 420 K, the C 1s feature shifts to increased binding energy, 284.2 eV, and its intensity significantly decreases. Consistent with TPD data, the CH_2S

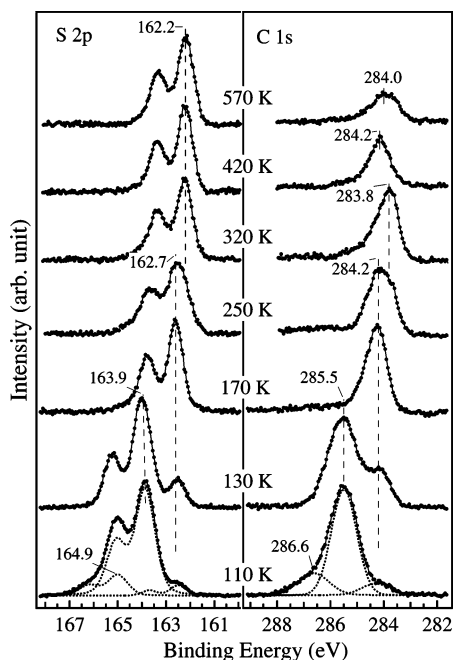


Figure 5. XPS spectra of S 2p and C 1s for a Pt(111) surface exposed to CH_3SH for 100 s at 110 K and subsequently heated to various temperatures.

species undergoes subsequent hydrogenation and dehydrogenation to desorb CH_4 and to form a surface CHS species.¹² At 570 K, the C 1s binding energy has a maximum at 284.0 eV, as obtained from the decomposition of CH_3I which forms a C adatom.²⁴ Hence, CHS decomposes to form surface C and S adatoms with the desorption of H_2 with a maximum at 475 K, as shown in Figure 3. On the basis of time-of-flight scattering and recoiling spectrometry (TOF-SARS) and normal incidence X-ray standing wave (NIXSW) results, the S adatom is proposed to reside on fcc 3-fold sites and the C adatom on hexagonal close-packed (hcp) 3-fold sites for the decomposition of $\text{CH}_3\text{-SH}$ on Pt(111).^{23,24}

To understand the effect of the length of the alkyl chain on the reaction pathways of alkanethiols on the Pt surface, we studied the adsorption and decomposition of $\text{C}_2\text{H}_5\text{SH}$ and $\text{C}_4\text{H}_9\text{-SH}$. Figure 6a shows composite TPD spectra for a Pt surface exposed to $\text{C}_2\text{H}_5\text{SH}$ at 110 K for 100 s. H_2 and C_2H_4 are the major desorption products of $\text{C}_2\text{H}_5\text{SH}$ decomposition. Two desorption features of C_2H_4 ($m/e = 28$) have maxima at 350 and 460 K. A small proportion of C_2H_6 ($m/e = 30$), a product of hydrogenation, is observed at temperatures of 250–370 K. The formation of C_2H_4 and C_2H_6 is observed only at large exposure. The desorption of H_2 as a function of $\text{C}_2\text{H}_5\text{SH}$ exposure is shown in Figure 6b. The temperature and features of H_2 desorption are similar to those obtained for CH_3SH , except for their relative intensities. Hence, $\text{C}_2\text{H}_5\text{SH}$ undergoes a mechanism of dehydrogenation similar to that of CH_3SH . The low-temperature desorption features at 170–370 K are due to recombination of surface hydrogen produced by sequential dehydrogenation of sulfhydryl and α -hydrogen of $\text{CH}_3\text{CH}_2\text{SH}$. Dehydrogenation of α -hydrogen results in the formation of $\text{CH}_3\text{-CHS}$ and CH_3CS intermediates, $\text{CH}_3\text{CH}_2\text{S} \rightarrow \text{CH}_3\text{CHS} \rightarrow \text{CH}_3\text{-CS}$. The intensity of the desorption feature at 275 K initially increases with increasing exposure. With exposures greater than 30 s, the peak intensity decreases with exposure, whereas the peak intensity at 225 K increases. This variation of intensity with exposure is due to competition of $\text{CH}_3\text{CH}_x\text{S}$ and hydrogen for adsorption sites. The high-temperature desorption at 420–500 K is attributed to further dehydrogenation of CH_3CS into

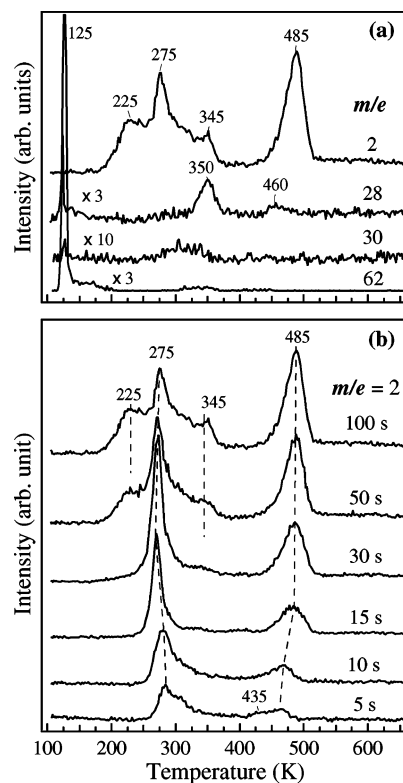


Figure 6. (a) Composite TPD spectra recorded from a Pt(111) surface exposed to $\text{C}_2\text{H}_5\text{SH}$ for 100 s at 110 K. (b) TPD spectra of H_2 for a Pt(111) surface exposed to $\text{C}_2\text{H}_5\text{SH}$ at 110 K as a function of duration of exposure.

surface carbon. This desorption signal shifts toward high temperature with increased exposure. The integrated intensity of the low-temperature desorption is significantly smaller than that for the case of CH_3SH , whereas the intensity of high-temperature desorption is larger.

Figure 7a shows composite TPD spectra for a Pt surface exposed to $\text{C}_4\text{H}_9\text{SH}$ at 110 K for 100 s. To obtain a high sensitivity of detection, we recorded the signals of $m/e = 41$ and 43 to monitor the formation of C_4H_8 and C_4H_{10} , which are the dominant fragments on ionization of C_4H_8 and C_4H_{10} , respectively. H_2 and C_4H_8 ($m/e = 41$) are the major desorption products of $\text{C}_4\text{H}_9\text{SH}$ decomposition. Two desorption features of C_4H_8 have maxima at 340 and 435 K. A trace proportion of C_4H_{10} ($m/e = 43$), a product of hydrogenation, is also formed in a temperature range similar to that of C_4H_8 desorption. C_4H_8 and C_4H_{10} are obtained only at large exposure. Figure 7b shows the desorption features of H_2 as a function of exposure to $\text{C}_4\text{H}_9\text{-SH}$. The desorption features are similar to those obtained for CH_3SH and $\text{C}_2\text{H}_5\text{SH}$, except for the desorption feature at ~ 405 K. This additional feature occurs only at small exposure, and its desorption temperature is similar to that of the dehydrogenation of a hydrocarbon on Pt(111).³³ Thus, this desorption is attributed to a surface $\text{C}_3\text{H}_7\text{CH}_x$ species formed upon breaking a $\text{C}_3\text{H}_7\text{CH}_x\text{-S}$ bond. At saturated coverage, two desorption signals appear at 450 and 480 K corresponding to the dehydrogenation of a $\text{C}_3\text{H}_7\text{CS}$ intermediate that is generated from the sequential elimination of α -hydrogen as proposed for the decomposition of CH_3SH and $\text{C}_2\text{H}_5\text{SH}$. The temperature of the latter feature is near those obtained for CH_3SH and $\text{C}_2\text{H}_5\text{SH}$, whereas the temperature of the former signal is less than the latter peak temperature by 30 K. Accordingly, these two desorption features are proposed to originate from the dehydrogenation of a $\text{C}_3\text{H}_7\text{CS}$ intermediate with two different adsorption conformations. One conformation has the alkyl group

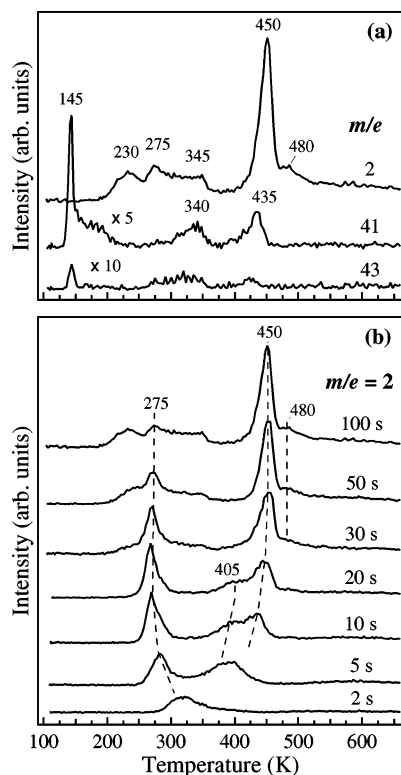
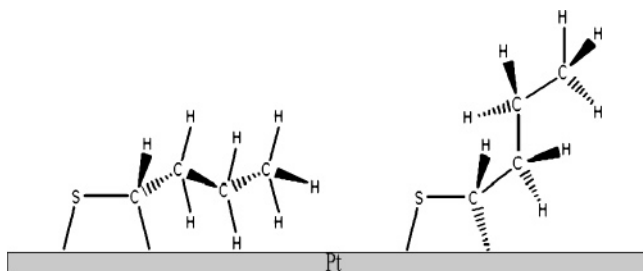


Figure 7. (a) Composite TPD spectra recorded from a Pt(111) surface exposed to C_4H_9SH for 100 s at 110 K. (b) TPD spectra of H_2 for a Pt(111) surface exposed to C_4H_9SH at 110 K as a function of duration of exposure.

lying on the surface; another has the alkyl group lying away from the surface. The schematics of the proposed conformations are depicted below.¹⁵



The C_3H_7CS intermediate with the second conformation decomposes to desorb hydrogen with a peak temperature at 480 K, as obtained for CH_3SH and C_2H_5SH . Alternatively, dehydrogenation of a C_3H_7CS intermediate with the former conformation might be facilitated through interaction between the surface and the hydrocarbon and can occur at a low temperature, corresponding to the desorption of H_2 at 450 K. This deduction is consistent with the decomposition of C_3H_7CS being determined by the C–H cleavage. Our TPD data show that most C_4H_9SH adsorbs on the surface with the former conformation.

As shown in Figures 3, 6, and 7, H_2 desorption obtained from the Pt surfaces saturated with CH_3SH , C_2H_5SH , and C_4H_9SH is similar for all three cases except for the relative intensities, although these alkanethiols differ in their alkyl group. The desorption features of H_2 at 170–370 K are attributed to the dehydrogenation of sulfhydryl and α -hydrogen that yields $R'-CS$ species which decompose further to desorb H_2 at 400–500 K. The intensity of the former H_2 desorption decreases with increasing length of the alkyl chain, whereas the latter desorption increases. The interaction between the long-chain alkyl group

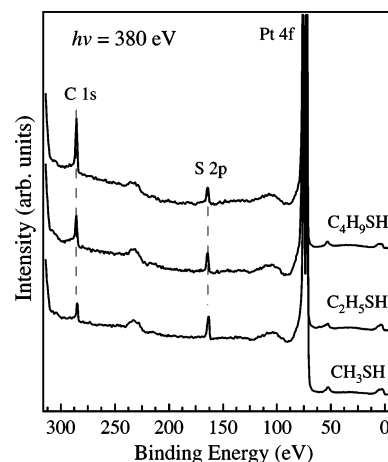


Figure 8. XPS spectra recorded for Pt surfaces exposed to (a) CH_3SH , (b) C_2H_5SH , and (c) C_4H_9SH for 100 s at 110 K and heated to 570 K. The photon energy used to collect these spectra is 380 eV.

and the surface decreases the density of adsorption and causes a decreased intensity of H_2 desorption at 170–370 K. However, the decomposition of an alkanethiol with a longer alkyl group results in an increased intensity of H_2 desorption at 400–500 K.

With sample annealing, the binding energies and intensities of S 2p and C 1s electrons for C_2H_5SH and C_4H_9SH are altered in a manner like that observed for CH_3SH . All chemisorbed C_2H_5SH and C_4H_9SH dissociates completely to form alkanethiolate at 170 K. At temperatures above 250 K, the intensity of the C 1s feature gradually decreases because of the desorption of products containing carbon, consistent with TPD data. Upon annealing to 570 K, all intermediate species decompose and yield atomic sulfur and carbon on the surface. Figure 8 shows XPS spectra recorded from a Pt surface saturated with CH_3SH , C_2H_5SH , and C_4H_9SH at 110 K and subsequently heated to 570 K to complete thermal decomposition. We reasonably assume that the density of adsorption of alkanethiol is proportional to the intensity of S 2p with respect to Pt 4f, as no species containing sulfur desorbs during thermal reaction. The intensity of the S 2p feature is decreased for an alkanethiol with a longer alkyl chain, whereas the intensity of the C 1s feature is increased. The density of adsorption decreases with increasing length of the chain of the alkyl group. In contrast, the saturation coverage remains constant on Ni(100) for alkanethiols with varied length of alkyl chain.¹⁵ The nature of the bond tethering the alkyl chains to a surface is an important factor in determining the orientation of an alkanethiolate adlayer. An alkanethiol adsorbs with a configuration in which the alkyl group interacts with the Pt surface and decreases its adsorption density. An alkanethiol with a longer alkyl chain leaves more residual carbon on the surface after thermal dehydrogenation, consistent with a greater intensity of H_2 desorption at 400–500 K.

As proposed above, C_4H_9SH adsorbs with a configuration in which the alkyl group interacts with the Pt surface. This interaction between the alkyl groups plays an important role and alters the adsorption orientation as the length of the alkyl chains increases.³⁵ The resulting adlayer of C_4H_9SH formed under a vacuum condition differs greatly from that obtained in solution, in which an alkanethiol with a longer alkyl group is orientated away from the surface.^{6,9,10} Thus, the orientation and structure of an adlayer on a substrate depends largely on the conditions of adsorption.³⁶

Our TPD and XPS data indicate that thermal reactions of C_2H_5SH and C_4H_9SH are analogous to those of CH_3SH . At small

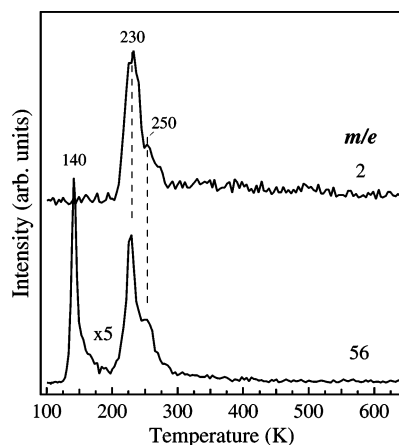


Figure 9. TPD spectra of H_2 ($m/e = 2$) and $\text{iso-C}_4\text{H}_8$ ($m/e = 56$) recorded from a Pt(111) surface exposed to $(\text{CH}_3)_3\text{CSH}$ at 110 K.

coverage, two shake-up peaks of C 1s are also observed at ~ 286.2 and ~ 287.1 eV at 300 and 320 K, respectively; they are attributed to the formation of π -bonded $\text{R}'\text{CH}=\text{S}$ and $\text{R}'\text{C}=\text{S}$ species via the elimination of α -hydrogen. According to our proposed mechanism, α -hydrogen is critical for the decomposition of $\text{R}'\text{CH}_2\text{S}$ to form a $\text{R}'\text{CS}$ species which decomposes further to desorb H_2 at 400–500 K. Figure 9 shows TPD spectra for a Pt surface exposed to *tert*-butylthiol ($(\text{CH}_3)_3\text{CSH}$), which has no α -hydrogen. A sharp feature with $m/e = 56$ at 145 K is due to the desorption and fragmentation of physisorbed *tert*-butylthiol. H_2 and $\text{iso-C}_4\text{H}_8$ (*iso*-butene; $m/e = 56$) are products of decomposition with an intense peak at 230 K and a shoulder feature at 250 K. The formation of $\text{iso-C}_4\text{H}_8$ is attributed to originate from breaking of the C–S bond and β -hydride elimination of $(\text{CH}_3)_3\text{CS}$: $(\text{CH}_3)_3\text{CS} \rightarrow (\text{CH}_3)_2\text{C}=\text{CH}_2 + \frac{1}{2}\text{H}_2 + \text{S}$. The desorption of H_2 accompanies the desorption of C_4H_8 , indicating that β -hydride elimination occurs about the desorption temperature of surface hydrogen. The width of the feature for H_2 desorption at 230 K is slightly greater than that of $\text{iso-C}_4\text{H}_8$. For the decomposition of *tert*-butylthiol, no H_2 desorption is observed at 400–500 K, which corresponds to the presence of a $\text{R}'\text{CS}$ species formed from the elimination of α -hydrogen. An α -hydrogen is evidently essential for the formation of a $\text{R}'\text{CS}$ species that can sustain up to 400 K.

Conclusions

Our TPD and XPS results elucidate the mechanism of thermal reaction of CH_3SH , $\text{C}_2\text{H}_5\text{SH}$, and $\text{C}_4\text{H}_9\text{SH}$ on a Pt surface. The extent of dissociation of alkanethiol, which yields alkanethiolate, is consistent with its acidity; an alkanethiol molecule with a shorter alkyl chain is more reactive to deprotonate on a Pt surface. All chemisorbed alkanethiols dissociate to form alkanethiolate at 170 K, which can undergo further dissociation of α -hydrogen to form $\text{R}'\text{CS}$ in a stepwise fashion: $\text{R}'\text{CH}_2\text{S} \rightarrow \text{R}'\text{CH}=\text{S} \rightarrow \text{R}'\text{CS}$, where $\text{R}' = \text{H}$, CH_3 , and C_3H_7 . H_2 is the only desorption product at small exposure. In addition to hydrogen, gaseous products containing carbon are also formed at high exposures, namely, CH_4 for CH_3SH , C_2H_4 and C_2H_6 for $\text{C}_2\text{H}_5\text{SH}$, and C_4H_8 and C_4H_{10} for $\text{C}_4\text{H}_9\text{SH}$. The $\text{R}'\text{CS}$ species further decomposes to desorb hydrogen at 400–500 K and forms sulfur and carbon on the surface. Two desorption features are observed at 450 and 480 K for the decomposition of $\text{C}_4\text{H}_9\text{SH}$, corresponding to a $\text{C}_3\text{H}_7\text{CS}$ intermediate with two adsorption configurations. $\text{C}_4\text{H}_9\text{SH}$ is proposed to adsorb mainly with a configuration in which the alkyl group interacts with the surface. This interaction between

the alkyl group and the surface diminishes the density of adsorption of alkanethiol but facilitates dehydrogenation of the $\text{R}'\text{CS}$ intermediate.

Our results provide information about the adsorption and thermal reaction of an alkanethiol on a Pt surface, when introduced onto the Pt surface through vapor deposition under UHV conditions. According to our proposed mechanisms for the decomposition of CH_3SH , $\text{C}_2\text{H}_5\text{SH}$, and $\text{C}_4\text{H}_9\text{SH}$, other thiols deprotonate to form a $\text{R}'\text{CS}$ layer that endures to only ~ 400 K, as they are used for a passivation or protection layer for a Pt surface or nanoparticle.

Acknowledgment. This work was supported by NSRRC and by National Science Council under grant NSC93-2113-M-003-012.

References and Notes

- (1) Speight, R. G. *The Chemistry and Technology of Petroleum*, 2nd ed.; Dekker: New York, 1991.
- (2) Rodriguez, J. A.; Kuhn, M.; Hrbek, J. *Chem. Phys. Lett.* **1996**, 251, 13.
- (3) Ulman, A. *Self-assembled Monolayers of Thiol Thin Films*; Academic Press: San Diego, CA, 1998; Vol. 24.
- (4) Ulman, A. *Chem. Rev.* **1996**, 96, 1533.
- (5) Whitesides, G. M.; Laibinis, P. E. *Langmuir* **1990**, 6, 87.
- (6) Stern, D. A.; Wellner, E.; Salaita, G. N.; Laguren-Davidson, L.; Lu, F.; Batina, N.; Frank, D. G.; Zapfen, D. C.; Walton, N.; Hubbard, A. T. *J. Am. Chem. Soc.* **1988**, 110, 4885.
- (7) Lang, P.; Mekhalif, Z.; Rat, B.; Garnier, F. *J. Electroanal. Chem.* **1998**, 441, 83.
- (8) Climent, V.; Rodes, A.; Albalat, R.; Claret, J.; Feliu, J. M.; Aldaz, A. *Langmuir* **2001**, 17, 8260.
- (9) Yang, Y. C.; Yen, Y. P.; Ou Yang, L. Y.; Yau, S. L.; Itaya, K. *Langmuir* **2004**, 20, 10030.
- (10) Li, Z.; Chang, S. C.; Williams, R. S. *Langmuir* **2003**, 19, 6744.
- (11) Tu, W.; Takai, K.; Fukui, K.; Miyazaki, A.; Enoki, T. *J. Phys. Chem. B* **2003**, 107, 10134.
- (12) Rufael, T. S.; Koestner, R. J.; Kollin, E. B.; Salmeron, M.; Gland, J. L. *Surf. Sci.* **1993**, 297, 272.
- (13) Koestner, R. J.; Stohr, J.; Gland, J. L.; Kollin, E. B.; Sette, F. *Chem. Phys. Lett.* **1985**, 120, 285.
- (14) Stöhr, J.; Jaeger, R. *Phys. Rev. B* **1982**, 26, 4111.
- (15) Parker, B.; Gellman, A. *Surf. Sci.* **1993**, 292, 223.
- (16) Friend, C. M.; Roberts, J. T. *Acc. Chem. Res.* **1988**, 21, 394.
- (17) Meagher, K. K.; Bocarsly, A. B.; Bernasek, S. L.; Ramanarayanan, T. A. *J. Phys. Chem. B* **2000**, 104, 3320.
- (18) Lai, Y. H.; Yeh, C. T.; Yeh, C. C.; Hung, W. H. *J. Phys. Chem. B* **2003**, 107, 9351.
- (19) Lai, Y. H.; Yeh, C. T.; Yeh, C. C.; Hung, W. H. *J. Phys. Chem. B* **2002**, 106, 5438.
- (20) Rieley, H.; Price, N. J.; White, R. G.; Blyth, R. I. R.; Robinson, A. W. *Surf. Sci.* **1995**, 331, 189.
- (21) Roberts, J. T.; Friend, C. M. *J. Phys. Chem.* **1988**, 92, 5205.
- (22) Jaffey, D. M.; Madix, R. J. *Surf. Sci.* **1994**, 311, 159.
- (23) Apai, G.; Baetzold, R. C.; Jupiter, P. J.; Viescas, A. J.; Lindau, I. *Surf. Sci.* **1983**, 134, 122.
- (24) Kim, S. S.; Kim, Y.; Kim, H. I.; Lee, S. H.; Lee, T. R.; Perry, S. S.; Rabalais, J. W. *J. Chem. Phys.* **1998**, 109, 9574.
- (25) Aplincourt, P.; Bureau, C.; Anthoine, J. L.; Chong, D. P. *J. Phys. Chem. A* **2001**, 105, 7364.
- (26) O'Shea, J. N.; Schnadt, J.; Brihwiler, P. A.; Hilleshejmer, H.; Mårtensson, N.; Patthey, L.; Krempasky, J.; Wang, C.; Luo, Y.; Ågren, H. *J. Phys. Chem. B* **2001**, 105, 1917.
- (27) Thomas, V. D.; Schwank, J. W.; Gland, J. L. *Surf. Sci.* **2001**, 501, 214.
- (28) Güttler, A.; Kolovos-Vellianitis, D.; Zecho, T.; Küppers, J. *Surf. Sci.* **2002**, 516, 219.
- (29) Koestner, R. J.; Salmeron, M.; Kollin, E. B.; Gland, J. L. *Chem. Phys. Lett.* **1986**, 125, 134.
- (30) Lee, J. J.; Fisher, C. J.; Bittencourt, C.; Woodruff, D. P.; Chan, A. S. Y.; Jones, R. G. *Surf. Sci.* **2002**, 516, 1.
- (31) Lin, T. H.; Huang, T. P.; Liu, Y. L.; Yeh, C. C.; Lai, Y. H.; Hung, W. H. *Surf. Sci.* **2005**, 578, 27.
- (32) Yang, M.; Somorjai, G. A. *J. Am. Chem. Soc.* **2004**, 126, 7698.
- (33) Bent, B. E. *Chem. Rev.* **1996**, 96, 1361 and references therein.
- (34) Zaera, F. *Acc. Chem. Res.* **1992**, 25, 260.
- (35) Bain, C. D.; Evall, J.; Whitesides, G. M. *J. Am. Chem. Soc.* **1989**, 111, 7155.
- (36) Zerulla, D.; Chassé, T. *Langmuir* **2002**, 18, 5392.